Electronic Supplementary Material (ESI) for Environmental Science: Processes & Impacts.

A prospective ecological risk assessment of high-efficiency III-V/silicon tandem solar cells

Supplementary Information

Blanco, C.F.[1*], Quik, J.T.K.[2], Hof, M.[2], Fuortes, A.[2], Behrens, P.[1], Cucurachi, S.[1], Peijnenburg, W.J.G.M.[1,2], Dimroth, F.[3], Vijver, M.G.[1]

[1] Institute of Environmental Sciences (CML), Leiden University. Box 9518, 2300 RA Leiden, The Netherlands
[2] National Institute of Public Health and the Environment (RIVM), P.O. Box 1, 3720 BA Bilthoven, The Netherlands
[3] Fraunhofer Institute for Solar Energy Systems, Heidenhofstr. 2, 79110 Freiburg, Germany
* Correspondence: c.f.blanco@cml.leidenuniv.nl

Table of Contents

1 Model overview

This risk assessment was conducted in five integrated steps:

- III-V/Si PV electricity demand scenarios: Projected the expected PV demand (in MW or GW) in each geographical scale over a period of 100 years using logistic growth curves.
- Dynamic stock flows: Determined the quantity of III-V/Si PV panels (in m^2 and GW of PV installation) manufactured, installed, and recycled/incinerated/landfilled in each year to meet the electricity demands of the previous step.
- Emissions: Determined the quantities of III-V materials emitted to the environment from III-V/Si PV panels at each life cycle stage.
    - *Manufacturing:* Emissions from this phase were deemed negligible as all waste goes to underground hazardous waste storage and/or is reused.
    - *Use phase*: Calculated the emissions that may occur from panel breakage which exposes the III-V materials in the PV cells to leaching during rain events.
    - *End-of-life phase*:
        - Recycling: no direct emissions to the environment were considered during PV materials separation and repurposing, only the generation of waste.
        - Incineration: Calculates emissions of III-V materials that vaporize and are not captured by the abatement system, escaping to air.
        - Landfilling: Calculates emissions from III-V materials that leach from the waste to the landfill leachate, and later escape the landfill through uncontrolled leakage to the surrounding soil. Also calculates emissions that can volatize to air in the landfill.
- Environmental fate: Models the distribution of emitted III-V materials (in kg) in each environmental compartment in each scale and calculates the predicted environmental concentrations (PEC) in each year.
- Risk Quotient: Evaluates the risk for a given year as a ratio of predicted environmental concentrations (PEC) to concentrations at which no observable effects are reported (PNEC).

These steps are described in detail in the following sections, along with the assumptions and calculation notes. The variable names used to represent the parameters in the model are provided below, and match the Excel spreadsheets and R scripts which are available for download at https://doi.org/10.5281/zenodo.7032993. The parameter values presented in each section below represent the base case, while most are subject to uncertainty and variability for which probability distributions were proposed as listed in Table S-2.

2 Demand scenarios

Demand scenarios for three geographical scales were modelled; one for Europe (continental, "EUR"), one for the city of Amsterdam (regional, "AMS"), and an intentionally loaded smaller area (~16 km^2) containing a floating utility-scale PV plant with surrounding rooftop PV and EOL treatment facilities within it (local, "LOC"). The scales are embedded in the model, so that the PV demand (and corresponding emissions) in the local scale is added to the regional scale, and the regional scale is added to the continental scale.

With an expected 28% panel conversion efficiency, III-V/Si panels will have a rating of 280 W_p/m^2. This is equivalent to the power output of the panel under standard irradiance conditions of 1000 W/m^2. The rating can also be expressed in terms of efficiency, as the ratio of power output to power input. To translate PV installed capacity to PV installation size (as total Area of panels, in m^2) we used Equation S-1.

$$Area = \frac{PV\ Capacity}{Rating} = \frac{PV\ Capacity}{efficiency \cdot 1000\ W/m^2} \qquad \text{(Eq. S-1)}$$

2.1 Continental scale: Europe

We modelled future electricity demand in Europe according to the Shell Sky Scenario[1], which sets the most ambitious targets for electrification and solar generation in Europe from the different scenarios presented by Shell. In this scale, total PV electricity demand would rise to 18.43 EJ (=5,138 TWh) by the year 2100, split equally between distributed and utility. Combining this with the IEA's "High GaAs" scenario[2] market shares where 15% of the utility share and 5% of the rooftop share would be taken by III-V/Si panels, the installed capacity of III–V/Si panels is 10%, or 513.8 TWh. We translate this electricity demand to installed capacity by assuming a 1200 kWh/kW_p average yield in Europe[3], although this can vary if the location of new PV installations shifts significantly to the north or south. Based on these data, we used a logistic growth curve[4] (equations S-2 and S-3) to project installed capacity at any given time $C(t)$, starting with an initial capacity addition of $C_0 = 100\ MW_p$ in the year 2031 and stabilizing at $C_f = 430\ GW_p$. We took the growth rate $k = 14.1\%$ from the 75th percentile of 1100 different PV deployment scenarios in Europe that were reviewed and harmonized by Jaxa-Rozen et. al.[5]

$$C(t) = \frac{C_f}{1 + A \cdot e^{-kt}} \qquad \text{(Eq. S-2)}$$

$$A = \frac{C_f - C_0}{C_0} \qquad \text{(Eq. S-3)}$$

Of the total amount of III-V/Si PV panels produced each year, we assumed 25% would be installed on rooftop installations, while 75% would be installed in utility-scale plants, following again the IEA's "High GaAs" scenario.[2] We further assumed that a fraction of utility-scale corresponding to 13.3% of utility (~10% of total generation) is supplied by floating structures on surface water bodies (lakes) based on projections made by Cazzaniga et al.[6] for floating PV installations. In lieu of data, we assumed an equal split between rooftop installations that drain to freshwater and those that drain to soil (Figure S-1).

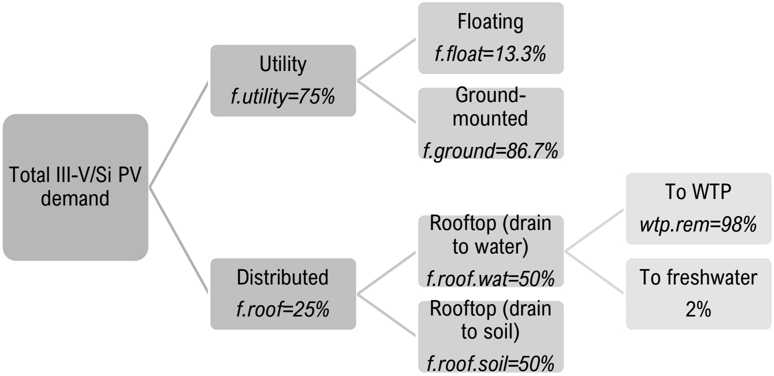

Fig S-1. Projected distribution of III-V/Si modules in Europe based on installation type and location.

2.2 Regional scale: Amsterdam area

The regional scale was modelled based on the stated policies of the Amsterdam municipality[7]. The number of installed solar panels has grown by approximately 50% annually from 2012 to mid-2019. The city's aspiration is to reach 550 MW by 2030, which is half of the total potential of roofs (large and small). Afterwards, the city is committed to "leave no roof unused", with a roof potential of 1100 MW. Floating PV and ground-based installations will be kept as an option only if the targets are not achievable otherwise. Following these stated aspirations, for this scale we assumed III-V/Si PV enters the market after 2030 with an initial installed capacity of 100 kWp and grows at the pace of 20% annually to take up 10% of the total rooftop potential. As per Equations S-2 and S-3, this can be represented by setting $C_0 = 0.1\ MW$, $C_f = 110\ MW$, and $k = 0.2$. The distribution of the panels according to type of installation are shown in Figure S-2.

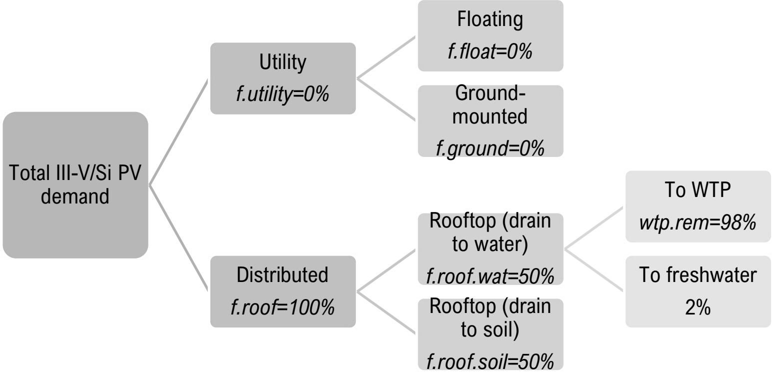

Fig S-2. Projected distribution of III-V/Si modules in Amsterdam based on installation type and location.

2.3 Local scale: Floating utility plant and surrounding rooftop installations

The third scale represents a very localized and hypothetical extreme situation, extrapolated from the current status (2020) of the Sloterplas lake area in Amsterdam. The number of rooftop panels currently installed in the encircled area (Figure S-3) is approximately 50,000. For this scale, we assume all the panels are replaced for III-V/Si panels in 2030. We also assumed all panels in this area will drain directly to soil, or towards the lake. In addition to this, 50 MW of III-V/Si panels are assumed to be installed in 2030 as a floating utility installation on the lake, taking up approximately 20% of the lake area.

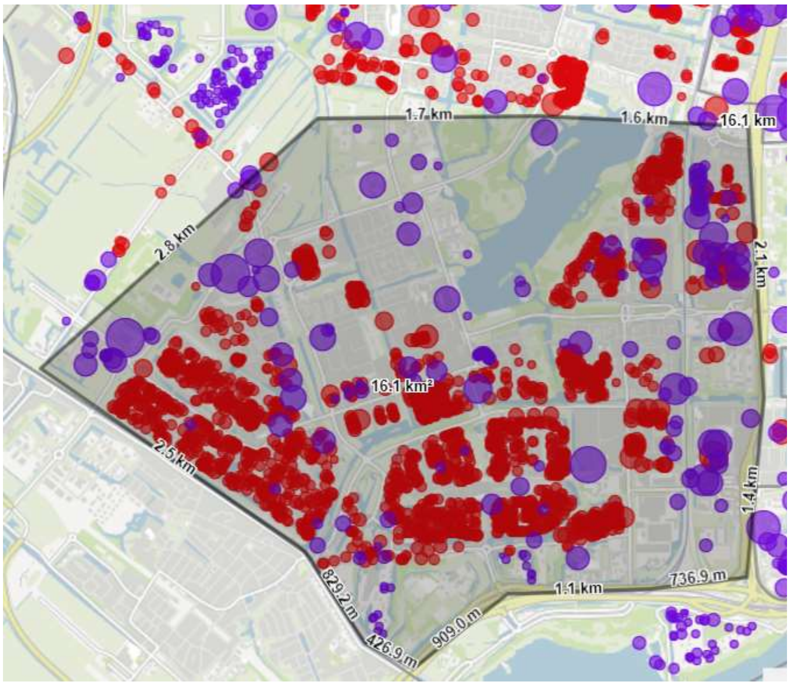

Fig S-3. Current PV installations around the Sloterplas lake in Amsterdam (red: on houses, purple: on non-houses or mixed).[*]

---

[*] https://maps.amsterdam.nl/zonnepanelen/?LANG=en.

3 Stock flows

Panel and waste stock flows are calculated on a yearly basis, accounting for the amount of panels that need to be manufactured to satisfy the installed capacity demand in each year. The yearly manufacturing requirements compensate for (i) increase in installed capacity, (ii) panels that are broken/damaged during use phase, and (iii) panels that reach the end their operational lifetime. The operational lifetime of panels varies for each yearly cohort according to an (assumed) normal distribution with mean = 30 years and standard deviation = 5 years.

According to current European Union regulations, 85% of solar panels by weight must be collected at EOL for recycling.[8] Current PV recycling practices largely focus on recovering the aluminum framing, circuitry and glass components of the panel while the cell is discarded. However, in Europe there are already ongoing pilots to recover silicon and valuable metals such as silver from the cells of conventional c-Si panels at industrial scale.[†] It is difficult to predict how fast similar recycling technologies may develop for III-V/Si cells. Based on interviews we conducted with recycling industry representatives in Europe, it is believed that 100 tons available for recycling each year could make arsenic recovery economically attractive. According to our stock model, such a quantity would become available at the European scale around the year 2100, which is still relatively early in the rapid exponential ramp-up in waste stocks (see Figure 1 in the main text). Recent regulatory trends are adding pressures to recover all metals and this is likely to push the feasibility date forward. Particularly in the Netherlands, the EOL management responsibilities for PV have been recently centralized on an organization (Stichting OPEN)[‡] which is already collecting a tariff from PV producers and importers to ensure financing will be available for high-quality recycling of future PV waste streams. No recovery of III-V materials is thus, in our view, an unlikely worst-case scenario that may only occur during the initial period while deployment is still very low.

Once III-V materials are recovered for reuse, we assume there will be a limiting recycling efficiency (*f.rec.reu=98%* in the base case*)* resulting in recycling rejects that unavoidably go to final disposal in incineration or landfill (*f.rec.rej=2%*). For the non-recycled materials (either not collected or not recovered during recycling), we consider that the final destination may be either direct landfilling or incineration. While PV waste generation, recycling and treatment data is reported in the official European database Eurostat[§], there is no disaggregated data for the specific treatment route (incineration vs. landfill). The ratio of landfilling to incineration of municipal waste – which may include small electronic devices- is reported[**], and varies from 100% to <1% across countries in Europe. Some countries like The Netherlands send most of their waste to incineration, although it has been reported that an important fraction of EOL PV panels is exported to Eastern Europe to extend their lifetimes albeit with lower performance. Due to the uncertainty and the different factors involved in deciding the ultimate destinations, we set the fraction of (non-recycled) shredded PV waste going to incineration in the Netherlands as 100% (no direct landfilling) and for Europe we use a PERT distribution with mean 50%, lower and upper parameters at 25% and 75% respectively.

In some cases, metals are recovered from incineration ash in Europe, but the most likely final destinations for the ash are reuse in road pavement and final landfilling. [9]

Figure S-4 depicts the different pathways to final destinations of III-V waste and the relative amounts in the base case scenario with recovery of III-V materials (NR) and a worst-case where III-V materials are not recovered (NR) during the modeling period.

[†] https://eitrawmaterials.eu/european-project-reprosolar-led-by-veolia-germany-will-test-full-photovoltaic-recycling-on-an-industrial-scale/

[‡] https://www.stichting-open.org/

[§] https://ec.europa.eu/eurostat/databrowser/view/ENV_WASELEEOS__custom_6231067/default/table?lang=en

[**] https://www.eea.europa.eu/data-and-maps/daviz/municipal-waste-landfill-rates-in#tab-chart_1

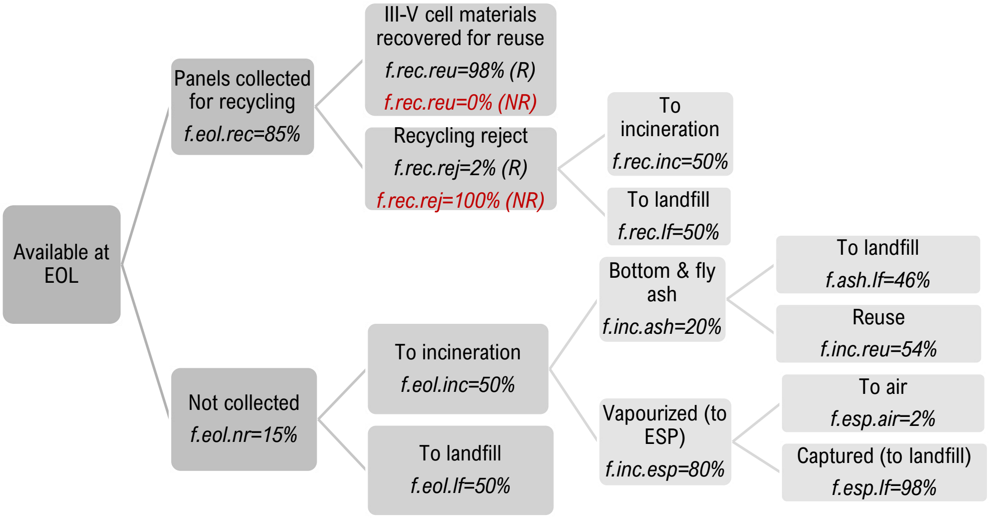

Fig S-4. Destination of III-V/Si panels at EOL. Percentage values represent the base (conservative) case with (R) and without (NR) arsenic recovery during recycling.

4 Emissions

4.1 Use phase[††]

The model supposes III-V materials emissions during the use phase may occur if there is leaching from broken panels during rain events. The potentially released amounts were determined by calculating the release per second per broken panel, and multiplying this by the exposure time to rainwater, number of panels, and fraction of panels with glass breakage. The release of arsenic/gallium/indium per broken panel is dependent on the speciation in the panel which consists of two factors: dissolution at the crack surface of directly exposed material (modelled according to Celik et al.[10]) and transport of arsenic on non-exposed parts that gets dissolved by water ingress and is transported to the crack where it is then released.

The total release can be expressed as:

$$R.system = \ (R.crack + trans.crack) \cdot t.exp \cdot n.system \cdot f.cracked \qquad \text{(Eq. S-4)}$$

Where:

R.system = total release of a metal from a specific speciation from the PV system in g/year

R.crack = dissolution rate of metal where the metal is directly exposed to the solvent due to the crack in g/s

trans.crack = transport of dissolved metal from the rest of the panel to the crack in g/s

t.exp = exposure time to solvent (rainwater) per year in s/year

n.system = number of panels in the PV system

f.cracked = fraction of panels in the system with glass panel breakage

The exposure time to solvent (rainwater) per year is calculated as:

$$t.exp \ = t.rain \ \cdot \ t.removal/365 \qquad \text{(Eq. S-5)}$$

[††] The "use phase" calculations presented in this section are based on the RIVM/Wageningen University and Research internship report by Matthias Hof, *"Environmental risk assessment of photovoltaic-panels applied on surface waters"* (April 15, 2021). Supervised by Joris Quik, Michiel van Kuppevelt (RIVM), Bart Koelmans (WUR).

Where:

t.rain = days of rain per year
t.removal = days until removal after breakage of panel

The dissolution rate of arsenic directly exposed at the cracks of a broken panel can be calculated as:[10]

$$R.crack = A.crack \cdot \left(\frac{D}{d}\right) \cdot (Cs - Cb) \qquad \text{(Eq. S-5)}$$

Where:

A.crack = cumulative surface area of cracks in m2
D = diffusion coefficient of metal in m2/s
d = thickness boundary layer of diffusion in m
Cs = saturated mass concentration of metal in water in g/m3
Cb = concentration of metal in bulk solvent (rainwater) in g/m3

In Equation S-5, the saturated mass concentration *Cs* is given by:

$$Cs = MW \cdot Ss \qquad \text{(Eq. S-6)}$$

Where:

MW = Molecular weight of metal atom in g/mol
Ss = saturated molar concentration of metal ions in mol/l

The saturated molar concentration *Ss* is:

$$Ss = \left(\frac{x}{y}\right)^{\frac{y}{x+y}} \cdot Ksp^{\frac{1}{x+y}} \qquad \text{(Eq. S-7)}$$

Where:

x = number of metal ions in soluble speciation
y = number of anions in soluble speciation
Ksp = solubility constant of soluble speciation

Finally, the cumulative crack surface is calculated as:

$$A.crack = n.cr \cdot (W.cr \cdot L.cr) \qquad \text{(Eq. S-8)}$$

Where:

n.cr = number of cracks
W.cr = width of the crack in m
L.cr = length of the crack in m

In addition to direct dissolution at the crack surface, III-V materials in the rest of the panel may be exposed to the solvent through the ingress of rainwater. We assumed that ingressed water is continuously present in the panel, and the concentration of dissolved III-V materials in the ingressed water was assumed to be saturated due to the long residence time. The release of metal through the crack can thus be described by the transport from its position in the panel to the crack through diffusion.

The transport of dissolved metal to crack is calculated as:

$$trans.crack = J.crack \cdot A.cr.sides \qquad \text{(Eq. S-9)}$$

Where:

J.crack = the flux of dissolved metal to the crack in $g/m^2/s$

A.cr.sides = the surface of the diffusion interface between the panel and the crack, which is the surface of the sides of the crack in m^2.

The flux of dissolved metal to crack is given by:

$$J.crack = D \cdot \frac{Cs-}{distance.cr} \qquad \text{(Eq. S-10)}$$

Where:

distance.cr = the average travel distance of the metal from any point in the panel to the crack

The surface of the diffusion interface can be calculated by the width and length of the crack, and the "depth" of the crack, or the thickness of the space between sheets of the panel through which the rainwater can ingress. Due to the possibility of multiple cracks on the panel, the total surface of the diffusion interface is the sum of the sides of multiple cracks. The total surface of the diffusion interface can be calculated as follows:

$$A.cr.sides = (n.cr \cdot 2(W.cr + L.cr) \cdot D.cr \qquad \text{(Eq. S-11)}$$

Where:

D.cr = depth of crack in m.

If the panel is regarded as a two-dimensional sheet, the average travel distance of dissolved metal from any point in the panel to the crack can be described by the average distance between two random points in a rectangle of a certain size. The average distance between two random points in a rectangle is described by Mathai et al.[11]:

$$\begin{aligned} avg.dis.panel = 1/15 \cdot ((L.panel^\wedge 3)/(W.panel^\wedge 2) + (W.panel^\wedge 3)/(L.panel^\wedge 2) \\ + d(-(L.panel^\wedge 2)/(W.panel^\wedge 2) - (W.panel^\wedge 2)/(L.panel^\wedge 2)) \\ + 5/2((W.panel^\wedge 2)/(A.panel)\ \ln((L.panel + LW)/(W.panel)) \\ + (L.panel^\wedge 2)/(W.panel)\ \ln((W.panel + LW)/(L.panel)))) \end{aligned} \qquad \text{(Eq. S-12)}$$

Where:

avg.dis.panel = the average distance between two random points in a rectangle with sides L.panel and W.panel in m

L.panel = the length of the panel in m

W.panel = the width of the panel in m

$LW = (L.panel^2 + W.panel^2)^{1/2}$

L.panel > W.panel

Because of the possibility of multiple cracks forming on the panel, the actual distance from any point on the panel to the crack would be smaller than the average distance between two points. As far as we are aware, there is no formula for the average distance between multiple random points in a rectangle. To approximate this decrease in distance with multiple cracks, the average distance calculated by Eq. S-12 was divided by the number of cracks on the panel:

$$distance.cr = \frac{avg.dis.panel}{n.cr} \qquad \text{(Eq. S-13)}$$

This underestimates the actual distance when cracks are not uniformly distributed, however this was deemed preferable over overestimating the distance as the latter leads to underestimating the release of metals and resulting ecotoxicological risk.

Finally, the amount of metal that can be released through direct dissolution at the crack with the Celik et al.[10] formula was limited to the amount of metal directly exposed to the outside environment (using an IF statement):

$$IF((R.crack \cdot t.exp) < Mu.crack; (R.crack \cdot t.exp); Mu.crack) \qquad \text{(Eq. S-14)}$$

The mass of metal directly exposed at crack is equal to:

$$Mu.crack = Mu.spec \cdot f.crack \qquad \text{(Eq. S-15)}$$

The amount of metal of specific speciation in panel is:

$$Mu.spec = Mu.PVarea \cdot L.panel \cdot W.panel \cdot f.spec \qquad \text{(Eq. S-16)}$$

The fraction of panel surface exposed by crack is:

$$f.crack = \frac{A.crack}{A.pv.panel} \qquad \text{(Eq. S-17)}$$

Where:

Mu.crack = amount of metal directly exposed to outside environment in g

Mu.spec = total weight of metal of specific speciation in panel in g

A.crack = total crack surface area in m2

Mu.PVarea = weight of metal per surface aera of PV panel in g/m2

f.spec = ratio of metal from specific speciation to total amount of that metal in the panel

Similarly, the total amount of metal that can be released from the panel trough dissolution in ingressed water and subsequent diffusion can be limited by:

$$IF((trans.crack \cdot t.exp) < Mu.ingress; (trans.crack \cdot t.exp); Mu.ingress) \qquad \text{(Eq. S-18)}$$

The amount of metal of specific speciation in panel that is not directly exposed by crack is:

$$Mu.ingress = Mu.PVarea \cdot A.pv.panel - Mu.crack \qquad \text{(Eq. S-19)}$$

Where:

Mu.ingress = weight of metal not directly exposed to outside environment in g.

4.2 End-of-life

4.2.1 Recycling

In the recycling scenario, we assumed that the current targets for collection and recovery set by European regulations would be fulfilled, i.e. 85% of panels were collected. Once collected, the methods available to recover III-V materials from similar technologies would be available (economically and technically) for large-scale implementation on III-V/Si cells. Such methods reported in patents and scientific literature indicate potential for between 90-99.9% recovery rates for the III-V materials. Particularly for the case of indium and gallium, recent concerns and regulatory trends around materials criticality are likely to create the incentives for high recovery rates. For a conservative approach, we take a uniform range of 90-99.9% recovery for all cases (indium, gallium, arsenic). In our model, the recovered amounts are thus retained in the economy (no further emissions to environmental compartments) and only the non-recoverable quantities of III-V materials during recycling ("recycling rejects") are then distributed to incineration or landfilling (see Figure S-4)

4.2.2 Landfilling

A simplified landfill model based on EPA's Composite Model for Leachate Migration with Transformation Products (EPACMTP)[12,13] was used to determine how much arsenic will dissolve from the PV discarded in landfills into the landfill leachate, and how much of the leachate containing these elements will escape the landfill into the surrounding environment. For simplicity, we assumed each cohort (yearly installation) will be disposed in a new landfill cell, all of which constitute monofills (only PV waste).

Once a landfill cell has been closed, it is expected that the concentration of an element in the leachate will decrease over time as the available quantity embedded in the waste is depleted. As per the EPACMTP model, this constitutes a "depleting source scenario", where the leachate concentration at a given time (t) is a linear function of the remaining concentration in the waste Cw(t):

$$C_L(t) = K_W \cdot C_W(t) \qquad \text{(Eq. S-20)}$$

In equation S-20, K_W is a waste/leachate partitioning coefficient. K_W values for arsenic were suggested by EPA[14], based largely on previously reported leachate extraction test results and modeling using the MINTEQA2 geochemical speciation model.

A mass balance can then be performed at any given time *t*, where the difference between the initial concentration in the waste and the concentration at time *t* should equal the total amount lost via leaching. Assuming all the waste is composed of the same PV waste (monofil), this mass balance can be expressed as:

$$A_W \cdot D_{LF} \cdot \rho_W \cdot \frac{dC_w}{dt} = A_W \cdot I \cdot C_L(t) \qquad \text{(Eq. S-21)}$$

C_W can be substituted for C_L using equation S-20 and equation S-21 can be rearranged to obtain:

$$\frac{dC_L}{dt} = \frac{-I}{D_{LF} \cdot \rho_W \cdot K_W} C_L \qquad \text{(Eq. S-22)}$$

Equation S-22 can be integrated to give:

$$C_L(t) = C_L^0 \cdot exp\left\{\left(\frac{-I}{D_{LF} \cdot \rho_W \cdot K_W}\right) t\right\} \qquad \text{(Eq. S-23)}$$

In equation S-23, C_L^0 represents the initial concentration of the element in the leachate at the time of landfill cell closure.

A small fraction of arsenic present in the landfill waste was assumed to be volatized due to biological processes. We took a range of values of 0.02-0.1% as reported by Webster et al.[15] for microbially mediated volatilization in anaerobic environments. It is likely that or monofils with reduced microbial activity this value is on the lower range if not negligible. This process is assumed to occur within the simulation time step of 1 year, and so is immediately subtracted from the amount available for leakage.

4.2.3 Incineration

During incineration, arsenic in PV waste can be reduced to bottom ash or volatized. In the latter case, it will join the flue gas which is mostly captured by an electrostatic precipitator (ESP) while a small fraction escapes to air. Arsenic in bottom ash and captured in the ESP (fly ash) are assumed to be sent to the same PV landfill cells used described in the previous section.

We based our assumptions on a study by Uryu et al.[16], who modelled the distribution of arsenic in GaAs FET semiconductors in mobile phones that are burned in hazardous waste incineration plants in Japan. Of the incinerated amount, 90% of arsenic was present in the gas phase at high incineration temperatures. 0.2% of arsenic present in the gas was found to escape to air while the remaining fraction (bottom ash and fly ash) was sent to a landfill.

5 Environmental fate

The landscape parameters in SimpleBox were compiled based on the EUSES model's database[17], which reflected the composition of the European Union ca. 2004. To match the projected PV demand which was taken for the EU in 2020, we adjusted the total continental area in SimpleBox and assumed that the fractions of water and soil remained constant. The emissions were sent to specific compartments in SimpleBox as indicated in Table S-1. As an additional adjustment, we directed the emissions to lakewater in the local scale to the freshwater compartment in SimpleBox to bypass inconsistencies in the original model. Thus, in the fate model lakewater and freshwater behave like a single freshwater compartment.

Table S-1 Receiving compartments for Use and EOL phase emissions

Emission	EUR	AMS	LOC
Use phase – leaching, utility (ground)	Continental agricultural soil, s2C	Regional agricultural soil, s2R	Local soil, sL
Use phase – leaching, utility (floating)	Continental freshwater, w1C	Regional freshwater, w1R	Local water, wL
Use phase – leaching, distributed	Continental freshwater, w1C	Regional freshwater, w1R	Local water, wL
EOL phase – incineration	Continental air, aC	Regional air, aR	Local air, aL
EOL phase – landfill leaching	Continental agricultural soil, s2C	Regional natural soil, s1R	Local soil, sL
EOL phase – landfill volatilization	Continental air, aC	Regional air, aR	Local air, aL

Table S-2 Model input parameters and uncertainty distributions

			EUR		AMS		LOC		
Model input parameter	Variable name	Units	Base value	Distribution parameters[‡‡]	Base value	Distribution	Base Value	Distribution	Refs.
--- *Installation parameters*									
Panel conversion efficiency	pv.eff	%	28%	P, a=25%, b=28%, c=31%	28%	P, a=25%, b=28%, c=31%	28%	P, a=25%, b=28%, c=31%	[18]
Panel lifetime	LT	years	30	N, μ=30, σ=5	30	N, μ=30, σ=5	30	N, μ=30, σ=5	[18]
Mass of element per m^2 cell: arsenic	m.PVarea	g/m^2	8.81	U, min=7.93, max=9.69	8.81	U, min=7.93, max=9.69	8.81	U, min=7.93, max=9.69	[§§]
Mass of element per m^2 cell: gallium	m.PVarea	g/m^2	15.06	U, min=13.55, max=16.57	15.06	U, min=13.55, max=16.57	15.06	U, min=13.55, max=16.57	
Mass of element per m^2 cell: indium	m.PVarea	g/m^2	0.02	U, min=0.018, max=0.022	0.02	U, min=0.018, max=0.022	0.02	U, min=0.018, max=0.022	
--- *Demand scenarios*									
Initial capacity addition	C0	MW	100	N/A	0.1	N/A	64	N/A	[***]
Carrying capacity	Cf	MW	4.3e5	N/A	110	N/A	64	N/A	[1,7]
Yearly growth rate	k	-	11.4%	N/A	20%	N/A	0	N/A	[5]
Fraction utility vs. rooftop	f.utility	-	75%	P, a=25%, b=75%, c=90%	10%	P, a=0, b=0.1, c=0.2	78.1%	N/A	[2]
Fraction utility floating vs. ground	f.float	-	13.3%	P, a=5%, b=13.3%, c=20%	13.3%	P, a=5%, b=13.3%, c=20%	100%	N/A	[6]
Fraction rooftop draining to water vs. soil	f.roof.wat	-	50%	P, a=10%, b=50%, c=90%	50%	P, a=10%, b=50%, c=90%	50%	P, a=10%, b=50%, c=90%	[†††]
Collected PV waste for recycling	f.EOL.rec	-	85%	U, min=85%, max=99.9%	85%	U, min=85%, max=99.9%	85%	U, min=85%, max=99.9%	[8]
Fraction of arsenic recovered for reuse	f.rec.reu	-	95%	U, min=90%, max=99.9%	95%	U, min=90%, max=99.9%	95%	U, min=90%, max=99.9%	[19–21]
Fraction of gallium recovered for reuse	f.rec.reu	-	95%	U, min=90%, max=99.9%	95%	U, min=90%, max=99.9%	95%	U, min=90%, max=99.9%	[19–21]

[‡‡] P: PERT, N: Normal, L: Lognormal, U: Uniform, T: Student's T, E: Exponential.

[§§] Internal calculations from the SiTaSol project (http://sitasol.com).

[***] Assumed

[†††] Assumed

			EUR		AMS		LOC		
Fraction of indium recovered for reuse	f.rec.reu	-	95%	U, min=90%, max=99.9%	95%	U, min=90%, max=99.9%	95%	U, min=90%, max=99.9%	19–21
Fraction not recycled to incinerator	f.EOL.inc	-	50%	P, a=25%, b=50%, c=75%	100%	N/A	100%	N/A	‡‡
--- *Use phase emissions*									
Yearly fraction of panels with breakage	f.cracked	-	0.06%	U, min=0% max=0.12%	0.06%	U, min=0% max=0.12%	0.06%	U, min=0% max=0.12%	22
Number of cracks per panel	n.cr		5	U, min=1 max=10	5	U, min=1 max=10	5	U, min=1 max=10	
Average width of crack	W.cr	mm	1	U, min=1 max=5	1	U, min=1 max=5	1	U, min=1 max=5	10
Average length of crack	L.cr	cm	10	P, a=1, b=10, c=30	10	P, a=1, b=10, c=30	10	P, a=1, b=10, c=30	
Average hours of rain per year	t.rain	h	840	P, a=240, b=840, c=1080	840	P, a=240, b=840, c=1080	840	P, a=240, b=840, c=1080	23
Diffusion coefficient of arsenic	Diff	m^2/s	1.2e-9	P, a=5e-10, b=1.2e-9, c=1.9e-9	1.2E-9	P, a=5e-10, b=1.2e-9, c=1.9e-9	1.2E-9	P: a=5e-10, b=1.2e-9, c=1.9e-9	24
Diffusion coefficient of gallium	Diff	m^2/s	7.9e-10	P, a=6e-10, b=7.9e-10, c=1.9e-9	7.9e-10	P, a=6e-10, b=7.9e-10, c=1.9e-9	7.9e-10	P, a=6e-10, b=7.9e-10, c=1.9e-9	25
Diffusion coefficient of indium	Diff	m^2/s	9.8e-10	P, a=6e-10, b=9.8e-10, c=1.9e-9	9.8e-10	P, a=6e-10, b=9.8e-10, c=1.9e-9	9.8e-10	P, a=6e-10, b=9.8e-10, c=1.9e-9	25
Thickness boundary layer of diffusion	d.panel	mm	0.01	U, min=0.01 max=0.1	0.01	U, min=0.01 max=0.1	0.01	U, min=0.01 max=0.1	10
Frac. rooftop drainage removed at WTP	wtp.rem	-	99%	U, min=98%, max=99.9%	99%	U, min=98%, max=99.9%	99%	U, min=98%, max=99.9%	26
--- *EOL phase emissions: landfill*									
Landfill cell depth	lf.d	m	2.9	E, λ=0.35	2.9	E, λ=0.35	2.9	E, λ=0.35	12
PV waste density (compacted)	waste.dens	kg/L	1.38	P, a=1, b=1.38, c=2	1.38	P, a=1, b=1.38, c=2	1.38	P, a=1, b=1.38, c=2	
Fraction of arsenic volatized in landfill	f.lf.air	-	0.065%	U, min=0.02% max=0.10%	0.065%	U, min=0.02% max=0.1%	0.065%	U, min=0.02% max=0.1%	15
Effective infiltration through landfill	lf.inf	m/yr	0.07	P, a=0, b=0.07, c=0.14	0.07	P, a=0, b=0.07, c=0.14	0.07	P, a=0, b=0.07, c=0.14	12

---

‡‡ Assumed

			EUR		AMS		LOC		
Waste/leachate partit. coefficient: As	K_W	L/kg	205	L, μ=205, σ=4.5	205	L, μ=205, σ=4.5	205	L, μ=205, σ=4.5	§§§
Waste/leachate partit. coefficient: Ga	K_W	L/kg	1,346	L, μ=1,346, σ=6.4	1,346	L, μ=1346, σ=6.4	1,346	L, μ=1346, σ=6.4	
Waste/leachate partit. coefficient: In	K_W	L/kg	2,800	L, μ=2,800, σ=2.9	2,800	L, μ=2,800, σ=2.9	2,800	L, μ=2,800, σ=2.9	
--- *EOL phase emissions: incineration*									
Fraction of arsenic volatized incinerator	f.inc.esp	-	50%	U, min=20%, max=80%	50%	U, min=20%, max=80%	50%	U, min=20%, max=80%	27
Fraction of gallium volatized incinerator	f.inc.esp	-	0%	None	0%	None	0%	None	16
Fraction of indium volatized incinerator	f.inc.esp	-	0%	None	0%	None	0%	None	16
ESP removal of volatized arsenic	f.esp.lf	-	99%	U, min=98%, max=99.99%	99%	U, min=98%, max=99.99%	99%	U, min=98%, max=99.99%	27
Fraction of incinerator ash to reuse	f.inc.reu	-	54%	P, a=0.25, b=0.54, c=0.75	54%	P, a=0.25, b=0.54, c=0.75	54%	P, a=0.25, b=0.54, c=0.75	9
--- *Substance parameters*									
Solid/water partitioning coefficient: As	Kp soil	L/kg	750	L, μ=750, σ=4.5	750	L, μ=750, σ=4.5	750	L, μ=750, σ=4.5	28
Solid/water partitioning coefficient: Ga	Kp soil	L/kg	11,000	L, μ=11,000, σ=6.4	11,000	L, μ=11,000, σ=6.4	11,000	L, μ=11,000, σ=6.4	28
Solid/water partitioning coefficient: In	Kp soil	L/kg	2,800	L, μ=2,800, σ=2.9	2,800	L, μ=2,800, σ=2.9	2,800	L, μ=2,800, σ=2.9	28
--- *Environmental fate: SimpleBox landscape & other parameters*									
Area of landscape covered by land	AREAland.	m^2	4.2E12	N/A	2.2E8	N/A	1.6E7	N/A	29
Area of landscape covered by sea	AREAsea.	m^2	4.2E12	N/A	0	N/A	N/A	N/A	29
Fraction of area freshwater	FRACfresh.	-	0.03	N/A	0.24	N/A	0.08	N/A	29

[§§§] Waste/leachate partitioning coefficients were calculated from the regression equation derived by Allison & Allison[14]: *log Kw = 0.7 log Kpsoil + 0.3*. The relation has a low correlation coefficient (R2 = 0.4) and the obtained values “must be regarded as highly uncertain”. To preserve correlations between Kw and Kpsoil, the Kpsoil (solid/water partitioning coefficient) values used in this formula in every model iteration were the same as those used in the SimpleBox fate model (see “Substance parameters” section in this Table).

			EUR		AMS		LOC		
Fraction of area natural soil	FRACnatsoil.	-	0.27	N/A	0	N/A	0	N/A	29
Fraction of area agricultural soil	FRACagsoil.	-	0.60	N/A	0.18	N/A	0	N/A	29
Fraction of area other soil	FRACothersoil.	-	0.70	N/A	0.58	N/A	0	N/A	29
Fraction of soil (local scale)	FRACsoil	-		N/A		N/A	0,92	N/A	29
Temperature	TEMP	°C	12	T, mix=-10, mode=12, max=35	12	T, mix=-10, mode=12, max=35	12	T, mix=-10, mode=12, max=35	30
Average wind speed	WINDspeed.	m/s	4.65	PERT, a=0, b=5.1, c=18	4.65	PERT, a=0, b=5.1, c=18	4.65	PERT, a=0, b=5.1, c=18	30
Mixed height air compartment	HEIGHT.a	m	605	T, min=77, mode=400, max=1338	605	T, min=77, mode=400, max=1338	605	T, min=77, mode=400, max=1338	30
Average rainfall	RAINrate.	mm/yr	925	PERT, a=350, b=700, c=2400	925	PERT, a=350, b=700, c=2400	925	PERT, a=350, b=700, c=2400	30
Average depth freshwater compartments	DEPTHfreshwater	m	4.7	PERT, a=1, b=3, c=15	2.6	PERT, a=1, b=3, c=5	4.7	PERT, a=1, b=3, c=15	30
Mixed depth of freshwater sediment	DEPTH.sd1	cm	4,7	T, min=1, mode=3, max=10	4,7	T, min=1, mode=3, max=10	4,7	T, min=1, mode=3, max=10	30
Mixed depth of marine sediment	DEPTH.sd2	cm	4,7	T, min=1, mode=3, max=10	N/A	N/A	N/A	N/A	30
Volume fraction water in soil	FRACw.s	-	0.29	T, min=0.003, mode=0.2, max=0.67		T, min=0.003, mode=0.2, max=0.67		T, min=0.003, mode=0.2, max=0.67	30
Volume fraction water in sediment	FRACw.sd	-	0.77	T, min=0.5, mode=0.8, max=0.999		T, min=0.5, mode=0.8, max=0.999		T, min=0.5, mode=0.8, max=0.999	30
Mass fraction organic carbon in suspended matter freshwater	CORG.susp1	-	0.1	L, μ=0.1, **σ**=0.04	0.1	L, μ=0.1, **σ**=0.04	0.1	L, μ=0.1, **σ**=0.04	30
Concentration suspended matter in freshwater	SUSP.w1	mg/L	24.4	L, μ=24.4, **σ**=23.5	24.4	L, μ=24.4, **σ**=23.5	24.4	L, μ=24.4, **σ**=23.5	30
Mass fraction organic carbon in suspended matter seawater	CORG.susp2	-	0.1	L, μ=0.1, **σ**=0.04	N/A	N/A	N/A	N/A	30
Concentration suspended matter in seawater	SUSP.w2	mg/L	24.4	L, μ=24.4, **σ**=23.5	N/A	N/A	N/A	N/A	30
Mass fraction organic carbon in freshwater sediment	CORG.sd1	-	0.05	L, μ=0.05, **σ**=0.04	0.05	L, μ=0.05, **σ**=0.04	0.05	L, μ=0.05, **σ**=0.04	30
Mass fraction organic carbon in sediment seawater	CORG.sd2	-	0.05	L, μ=0.05, **σ**=0.04	N/A	N/A	N/A	N/A	30

			EUR		AMS		LOC		
Mass fraction organic carbon in soil	CORG.s	-	0.05	L, μ=0.05, σ=0.04	0.05	L, μ=0.05, σ=0.04	0.05	L, μ=0.05, σ=0.04	30
Deposition velocity aerosol particles	AEROSOLdeprate	m/s	1.0E-3	L, μ=1.0E-3, σ=1.0E-3	1.0E-3	L, μ=1E-3, σ=1.0E-3	1.0E-3	L, μ=1.0E-3, σ=1.0E-3	30
Aerosol collection efficiency	COLLECTeff	-	2.0E4	T, min=5.0E3, mode=2.0E4, max=3.5E4	2.0E4	T, min=5.0E3, mode=2.0E4, max=3.5E4	2.0E4	T, min=5.0E3, mode=2.0E4, max=3.5E4	30
Settling velocity suspended particles	SETTLvelocity	m/s	2.1E-5	T, mix=3.0E-6, mode=2.9E-5, max=3.0E-5	2.1E-5	T, mix=3.0E-6, mode=2.9E-5, max=3.0E-5	2.1E-5	T, mix=3.0E-6, mode=2.9E-5, max=3.0E-5	30
Autochtonous production of suspended matter in freshwater	PRODsusp.w1	g/m^2/yr	12	T, min=5, mode=10, max=20	12	T, min=5, mode=10, max=20	12	T, min=5, mode=10, max=20	30
Autochtonous production of suspended matter in seawater	PRODsusp.w2	g/m^2/yr	1.2	T, min=0.5, mode=1.0, max=2.0	N/A	N/A	N/A	N/A	30
Partial mass transfer coefficient water side of water/sediment interface	Kwsd.water.w	m/s	4.0E-6	T, min=2.78E-6/3, mode=2.78E-6, max=2.78E-6*3	4.0E-6	T, min=2.78E-6/3, mode=2.78E-6, max=2.78E-6*3	4.0E-6	T, min=2.78E-6/3, mode=2.78E-6, max=2.78E-6*3	30
Partial mass transfer coefficient sediment side of water/sediment interface	Kwsd.sed.sd	m/s	4.0E-8	T, min=2.78E-8/3, mode=2.78E-8, max=2.78E-8*3	4.0E-8	T, min=2.78E-8/3, mode=2.78E-8, max=2.78E-8*3	4.0E-8	T, min=2.78E-8/3, mode=2.78E-8, max=2.78E-8*3	30
Erosion of soil	EROSION.s	mm/yr	0.03	T, min=0, mode=0.03, max=0.06	0.03	T, min=0, mode=0.03, max=0.06	0.03	T, min=0, mode=0.03, max=0.06	30
Volume fraction of precipitation on soil running off to surface water	FRACrun.s	-	0.25	T, min=0, mode=0.25, max=0.50	0.25	T, min=0, mode=0.25, max=0.50	0.25	T, min=0, mode=0.25, max=0.50	30
Volume fraction of precipitation infiltrating into soil	FRACinf.s	-	0.25	T, min=0, mode=0.25, max=0.50	0.25	T, min=0, mode=0.25, max=0.50	0.25	T, min=0, mode=0.25, max=0.50	30
Mineral density sediment and soil	RHOsolid	Kg/m^3	2.5E3	T, min=2.0E3, mode=2.5E3, max=3.0E3	2.5E3	T, min=2.0E3, mode=2.5E3, max=3.0E3	2.5E3	T, min=2.0E3, mode=2.5E3, max=3.0E3	30

6 References

1. Shell International B.V. Sky Scenario. *Shell Scenarios SKY Meeting the Goals of the Paris Agreement* https://www.shell.com/energy-and-innovation/the-energy-future/scenarios/shell-scenario-sky.html (2018).
2. IEA. *The Role of Critical Minerals in Clean Energy Transitions.* (2021).
3. Global Solar Atlas. https://globalsolaratlas.info/map?c=50.958427,15.512695,4&s=47.338823,5.976563&m=site.
4. Kucharavy, D. & De Guio, R. Logistic substitution model and technological forecasting. in *Procedia Engineering* vol. 9 (2011).
5. Jaxa-Rozen, M. & Trutnevyte, E. Sources of uncertainty in long-term global scenarios of solar photovoltaic technology. *Nat Clim Chang* **11**, 266–273 (2021).
6. Cazzaniga, R. & Rosa-Clot, M. The booming of floating PV. *Solar Energy* **219**, 3–10 (2021).
7. City of Amsterdam. Policy: Renewable energy. *Policy: Sustainability and energy* https://www.amsterdam.nl/en/policy/sustainability/renewable-energy/.
8. European Parliament; Council of the European Union. *Directive 2012/19/EU of the European Parliament and of the Council of 4 July 2012 on waste electrical and electronic equipment (WEEE).* (2012). doi:10.3000/19770677.L_2012.197.eng.
9. Blasenbauer, D. *et al.* Legal situation and current practice of waste incineration bottom ash utilisation in Europe. *Waste Management* **102**, 868–883 (2020).
10. Celik, I., Song, Z., Phillips, A. B., Heben, M. J. & Apul, D. Life cycle analysis of metals in emerging photovoltaic (PV) technologies: A modeling approach to estimate use phase leaching. *J Clean Prod* **186**, 632–639 (2018).
11. Mathai, A. M., Moschopoulos, P. & Pederzoli, G. Random points associated with rectangles. *Rendiconti del Circolo Matematico di Palermo* **48**, 163–190 (1999).
12. U.S. Environmental Protection Agency Office of Solid Waste. *EPA's Composite Model for Leachate Migration with Transformation Products (EPACMTP) Parameters/Data Background Document.* (2003).
13. U.S. Environmental Protection Agency Office of Solid Waste. *EPA's Composite Model for Leachate Migration with Transformation Products (EPACMTP) Technical Background Document.* (2003).
14. Allison, J. D. & Allison, T. L. *Partitioning Coefficients for Metals in Surface Water, Soil and Waste.* https://cfpub.epa.gov/si/si_public_record_report.cfm?Lab=NERL&dirEntryId=135783 (2005).
15. Webster, T. M. *et al.* Anaerobic Disposal of Arsenic-Bearing Wastes Results in Low Microbially Mediated Arsenic Volatilization. *Environ Sci Technol* **50**, 10951–10959 (2016).
16. Uryu, T., Yoshinaga, J. & Yanagisawa, Y. Environmental Fate of Gallium Arsenide Semiconductor Disposal. *J Ind Ecol* **7**, 103–112 (2003).

17. J.P.A. Lijzen and M.G.J. Rikken (eds.). *European Union System for the Evaluation of Substances 2.0 (EUSES 2.0).* https://echa.europa.eu/documents/10162/6177702/euses_2-1_background_document_en.pdf/51d73868-784b-1476-f201-8a4ba17e78e0 (2004).

18. Blanco, C. F. *et al.* Environmental impacts of III–V/silicon photovoltaics: life cycle assessment and guidance for sustainable manufacturing. *Energy Environ Sci* **13**, 4280–4290 (2020).

19. Zhan, L., Wang, Z., Zhang, Y. & Xu, Z. Recycling of metals (Ga, In, As and Ag) from waste light-emitting diodes in sub/supercritical ethanol. *Resour Conserv Recycl* **155**, (2020).

20. Van Den Bossche, A., Vereycken, W., Vander Hoogerstraete, T., Dehaen, W. & Binnemans, K. Recovery of Gallium, Indium, and Arsenic from Semiconductors Using Tribromide Ionic Liquids. *ACS Sustain Chem Eng* **7**, 14451–14459 (2019).

21. Zhan, L., Xia, F., Xia, Y. & Xie, B. Recycle Gallium and Arsenic from GaAs-Based E-Wastes via Pyrolysis-Vacuum Metallurgy Separation: Theory and Feasibility. *ACS Sustain Chem Eng* **6**, 1336–1342 (2018).

22. Köntges, M. *et al. Review of Failures of Photovoltaic Modules.* https://iea-pvps.org/wp-content/uploads/2020/01/IEA-PVPS_T13-01_2014_Review_of_Failures_of_Photovoltaic_Modules_Final.pdf (2014).

23. Hosseinzadehtalaei, P., Tabari, H. & Willems, P. Climate change impact on short-duration extreme precipitation and intensity–duration–frequency curves over Europe. *J Hydrol (Amst)* **590**, 125249 (2020).

24. Tanaka, M. *et al.* The difference of diffusion coefficients in water for arsenic compounds at various pH and its dominant factors implied by molecular simulations. *Geochim Cosmochim Acta* **105**, 360–371 (2013).

25. Vanýsek, P. Ionic conductivity and diffusion at infinite dilution. in *Handbook of Chemistry and Physics* (5-111)-(5-113) (CRC Press, 1992).

26. Sun, L., Lu, M., Li, Q., Jiang, H. & Yin, S. Research progress of arsenic removal from wastewater. *IOP Conf Ser Earth Environ Sci* **218**, 012142 (2019).

27. Jung, C. H., Matsuto, T., Tanaka, N. & Okada, T. Metal distribution in incineration residues of municipal solid waste (MSW) in Japan. *Waste Management* **24**, 381–391 (2004).

28. Sheppard, M. I., Sheppard, S. C. & Grant, C. A. Solid/liquid partition coefficients to model trace element critical loads for agricultural soils in Canada. *Can J Soil Sci* **87**, 189–201 (2007).

29. Vermeire, T. G. *et al.* European Union System for the Evaluation of Substances (EUSES). Principles and structure. *Chemosphere* **34**, 1823–1836 (1997).

30. Bakker, J., Brandes, L. J., den Hollander, H. A., van de Meent, D. & Struijs, J. *Validating SimpleBox-Computed Steady-state Concentration Ratios.* (2003).